COVID-19 LOCKDOWNS REVEAL PRONOUNCED DISPARITIES IN NITROGEN DIOXIDE POLLUTION LEVELS

GAIGE HUNTER KERR[1], DANIEL L. GOLDBERG[1,2], SUSAN C. ANENBERG[1]

[1] *Department of Environmental and Occupational Health, Milken Institute School of Public Health, George Washington University, Washington, DC, 20052 USA,*
[2] *Energy Systems Division, Argonne National Laboratory, Lemont, IL, 60439 USA*

1. Abstract

The unequal spatial distribution of ambient nitrogen dioxide (NO_2), an air pollutant related to traffic, leads to higher exposure for minority and low socioeconomic status communities. We exploit the unprecedented drop in urban activity during the COVID-19 pandemic and use high-resolution, remotely-sensed NO_2 observations to investigate disparities in NO_2 levels across different demographic subgroups in the United States. We show that COVID-19 lockdowns reduced, but did not eliminate, the overall racial, ethnic, and socioeconomic NO_2 disparities. Prior to the pandemic, satellite-observed NO_2 levels in the least white census tracts of the United States were double NO_2 levels in the most white tracts. During the pandemic, the largest lockdown-related NO_2 reductions occurred in urban neighborhoods that have 30% fewer white residents and 111% more Hispanic residents than neighborhoods with the smallest reductions, likely driven by the greater density of highways and interstates in these racially and ethnically diverse areas. However, the least white tracts still experienced ∼50% higher NO_2 levels during the lockdowns than the most white tracts experienced prior to the pandemic. Future policies aimed at eliminating pollution disparities will need to look beyond reducing emissions from only passenger traffic and also consider other collocated sources of emissions such as heavy-duty trucks, power plants, and industrial facilities.

2. Significance Statement

We leverage the unparalleled changes in human activity during COVID-19 and the unmatched capabilities of the TROPOspheric Monitoring Instrument to understand how lockdowns impact ambient nitrogen dioxide (NO_2) pollution disparities

E-mail address: gaigekerr@gwu.edu.

in the United States. The least white communities experienced the largest NO_2 improvements during lockdowns; however, disparities between the least and most white communities are so large that the least white communities still faced higher NO_2 levels during lockdowns than the most white communities experienced prior to lockdowns, despite a $\sim$ 50% reduction in passenger vehicle traffic. Similar findings hold for ethnic, income, and educational attainment subgroups. Future strategies to reduce NO_2 disparities will need to target emissions from not only passenger vehicles but other collocated on-road and stationary sources.

3. Introduction

Adverse air quality is an environmental justice issue as it disproportionately affects lower income, minority, and marginalized populations around the world [Bell and Ebisu, 2012, Landrigan et al., 2018, Schell et al., 2020]. Growing evidence suggests that these populations experience more air pollution than is caused by their consumption [Nguyen and Marshall, 2018, Tessum et al., 2019, Sergi et al., 2020]. Within the United States (U.S.), disparities in exposure are persistent, despite successful regulatory measures that have reduced pollution [Clark et al., 2017, Colmer et al., 2020]. Nitrogen dioxide (NO_2) is a short-lived trace gas formed shortly after fossil fuel combustion and regulated by the National Ambient Air Quality Standards under the Clean Air Act. Exposure to NO_2 is associated with a range of respiratory diseases and premature mortality [Jerrett et al., 2013, Anenberg et al., 2018, Achakulwisut et al., 2019]. NO_2 is also a precursor to other pollutants such as ozone and particulate matter [Stohl et al., 2015]. Major sources of anthropogenic NO_2, such as roadways and industrial facilities, are often located within or nearby minority and disenfranchised communities [Mohai et al., 2009, Rowangould, 2013], and disparities in NO_2 exposure across demographic subgroups have been the focus of several recent studies [Hajat et al., 2013, Clark et al., 2014, Clark et al., 2017, Demetillo et al., 2020].

In early 2020, governments around the world imposed lockdowns and shelter-in-place orders in response to the spread of the coronavirus disease 2019 (COVID-19). The earliest government-mandated lockdowns in the U.S. began in California on 19 March 2020, and many states followed suit in the following days. Changes in mobility patterns indicate that self-imposed social distancing practices were underway days to weeks before the formal announcement of lockdowns [Badr et al., 2020]. Lockdowns led to sharp reductions in surface-level NO_2 [He et al., 2020, Shi and Brasseur, 2020, Venter et al., 2020] and tropospheric column NO_2 measured from satellite instruments [Bauwens et al., 2020, Goldberg et al., 2020b] over the U.S., China, and Europe. According to government-reported inventories, roughly 60% of anthropogenic emissions of nitrogen oxides ($NO_x \equiv NO + NO_2$) in the U.S. in 2010 were emitted by on-road vehicles [US Environmental Protection Agency, 2015], and up to 80% of ambient NO_2 in urban areas can be linked to traffic emissions [Levy et al., 2014, Sundvor et al., 2013]. As such, NO_2 is often used as a marker for road traffic in urban areas. Multiple lines of evidence such as seismic quieting and reduced mobility via location-based services point to changes in traffic-related emissions as the main driver of drops in NO_2 pollution during lockdowns due to the large proportion of the population working from home [Diffenbaugh et al., 2020, Lecocq et al., 2020, Venter et al., 2020].

Here we exploit the unprecedented changes in human activity unique to the COVID-19 lockdowns and remotely-sensed NO_2 columns with unprecedented spatial resolution and coverage to understand inequalities in the distribution of NO_2 pollution for different racial, ethnic, and socioeconomic subgroups in the U.S. Specifically, we address the following: Which demographic subgroups received the largest NO_2 reductions? Did the lockdowns grow or shrink the perennial disparities in NO_2 pollution across different demographic subgroups? Although the lockdowns are economically unsustainable, how can they advance environmental justice and equity by informing long-term policies to reduce NO_2 disparities and the associated public health damages?

4. Results

Previous studies examining satellite-derived NO_2 found the highest levels in urban areas [Krotkov et al., 2017, Goldberg et al., 2020a], and we find that these areas clearly stand out as NO_2 hotspots during our baseline period (Figure 1a). NO_2 column densities averaged over all urban areas are a factor of two higher than over rural areas during the baseline period. Absolute differences in NO_2 between the baseline and lockdown periods ("drops") show sharp decreases over virtually all major metropolitan regions (Figure 1b). Outside of metropolitan areas, we note smaller NO_2 drops in Appalachia and the South, likely stemming from a combination of lockdown-related changes in traffic emissions as well as favorable weather [Goldberg et al., 2020b]. Parts of the Great Plains and Midwest experience slight increases in NO_2 during lockdowns ($< 0.5 \times 10^{15}$ molecules cm^{-2}), which could reflect differences in natural (e.g., soil, lightning, stratospheric NO_x) or anthropogenic sources of NO_2 between the baseline and lockdown periods. Given that the largest lockdown-related changes in NO_2 occur in urban areas and to avoid urban-rural demographic gradients, we primarily focus on urban NO_2 changes and how these changes impact different demographic subgroups in urban areas.

The largest urban NO_2 drops occur in census tracts that are more non-white and Hispanic and have a higher proportion of their population without a vehicle or a post-secondary education compared with tracts with the smallest drops (Figure 1d-h). The percentage of white residents in tracts with the largest drops in NO_2 is 30% less compared with tracts with the smallest drops, which represent a slight increase over baseline levels (Figure 1g). The percentage of Hispanic- or Latinx-identifying residents in tracts with the largest drops is 111% larger than tracts with the smallest drops (Figure 1d). This pattern found in urban tracts also holds in all

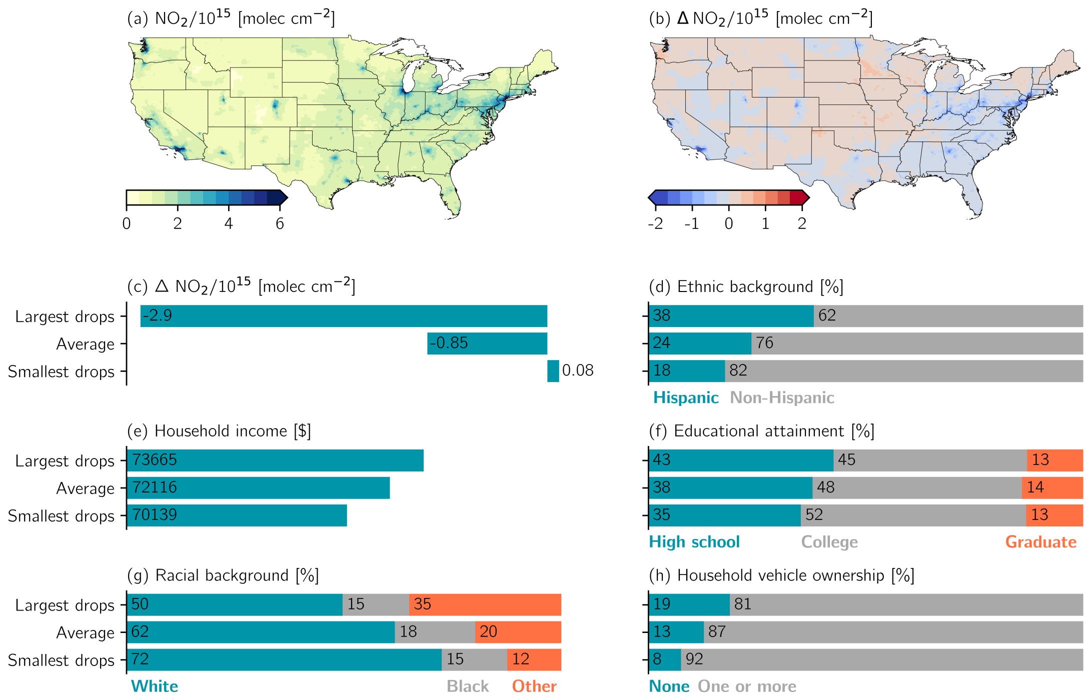

FIGURE 1. **Spatial distribution of NO_2 columns during the baseline and COVID-19 lockdown periods and apportionment of drops among different demographic subgroups.** (a) Census-tract average baseline NO_2 (13 March-13 June 2019). (b) Absolute difference between lockdown (13 March - 13 June 2020) and baseline NO_2 (Δ NO_2), where Δ $NO_2 < 0$ corresponds to NO_2 drops during lockdowns. (c) Demographic data averaged over urban tracts with the largest drops (Δ NO_2 in first decile), all urban tracts, and urban tracts with the smallest drops (Δ NO_2 in the tenth decile).

(urban and rural) tracts and rural tracts, despite the different socio-demographic composition of the population in these areas (compare Figures 1 and S1).

Since less educated communities and communities with a large proportion of racial and ethnic minorities have faced higher levels of NO_2 and other pollutants for decades [Hajat et al., 2013, Hajat et al., 2015, Clark et al., 2017, Colmer et al., 2020, Schell et al., 2020], it is surprising that these communities experienced the largest drops in NO_2 pollution during COVID-19 lockdowns. However, Figure 1 does not indicate how lockdown-related NO_2 drops grew or shrunk disparities, and we next examine disparities in baseline and lockdown NO_2 in the most advantaged versus disadvantaged census tracts in the U.S.

In the baseline period, low income, less educated neighborhoods and those with a higher proportion of minority residents consistently face higher levels of NO_2 among all urban tracts across the U.S. and in nearly all 15 major metropolitan statistical areas (MSAs) explored (Figure 2). An unexpected finding is that tracts with the highest income and educational attainment in rural areas and aggregated over both rural and urban areas have higher NO_2 levels than tracts with the lowest income or educational attainment (Figure 2). When considering all census tracts (both urban and rural), the most pronounced disparities are on the basis of race and ethnicity: the least white tracts and most Hispanic tracts have 2.1 and 1.9 times greater baseline NO_2 levels than the most white and least Hispanic tracts, respectively (Figure 2a, S2g). These disparities persist when examining the individual MSAs in the U.S. For example, baseline NO_2 in tracts with the lowest median household income in New York and Los Angeles is 1.6 and 1.7 times higher, respectively, than tracts with the highest income (Figure 2b).

The unprecedented change in human activity during COVID-19 lockdowns narrowed disparities in NO_2 across demographic subgroups in the U.S. (Figures 2, S2). The ratio of NO_2 in the least white urban tracts to NO_2 in the most white urban tracts in the U.S. decreased from 1.51 prior to the lockdowns to 1.36 during the lockdowns (Figure 2a). Individual MSAs such as New York, Los Angeles, and Atlanta undergo even more striking reductions in their racial, income, and educational attainment disparities. There are some cities or aggregations, however, where disparities remain constant or even grow during lockdowns. As examples: the ratio of NO_2 in all urban tracts with the lowest income to those with the highest income grows from unity prior to the lockdowns to 1.06 during the lockdowns (Figure 2b), and the magnitude of disparities across demographic subgroups is relatively constant in Phoenix (Figure 2).

Although the short-term changes in NO_2 during lockdowns reduced disparities, the most exposed demographic subgroups prior to the lockdowns remained so during the lockdowns (Figure 2, S2). For example, the racial disparities were so large during the baseline period that even the unprecedented drop in human activity during lockdowns did not bring NO_2 levels for the least white tracts down to the levels experienced by the most white tracts prior to the lockdowns. The same patterns hold true on the bases of ethnicity, income, and educational attainment (Figures 2, S2). These results are neither an artifact of how we defined demographic subgroups (Figure S2) or the precise time period over which we characterize disparities (Figure S3).

Within urban areas, we find that the magnitude of NO_2 drops is tightly coupled to the density of nearby primary roads (highways and interstates). The density of primary roads in urban tracts with the largest NO_2 drops is six times greater than in urban tracts with the smallest NO_2 drops (Figure 3). The racial, ethnic, income, and educational composition of tracts are also closely related to primary road density; urban tracts with lower income and vehicle ownership and a larger

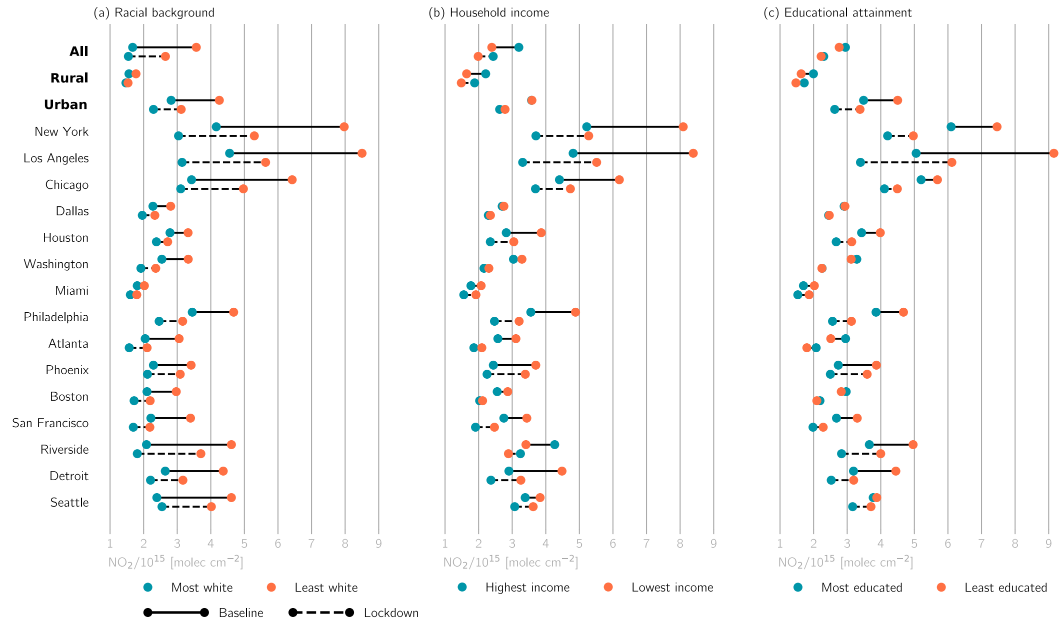

FIGURE 2. **Disparities in baseline and lockdown NO_2 columns across different demographic subgroups.** Subgroups are determined by identifying census tracts with extreme values for each demographic variable, and NO_2 levels are averaged over all, rural, and urban tracts with these extreme values. Urban tracts are further separated into the fifteen largest MSAs listed on the vertical axis.

percentage of racial and ethnic minorities are located near a higher density of primary roads (Figure 3). The difference in primary road density on the basis of vehicle ownership is especially stark: tracts with the lowest vehicle ownership (i.e., tracts in the first decile) have ~ 9.5 times higher primary road density than tracts with the highest ownership (i.e., tenth decile). Similarly, the least white tracts have a primary road density ~ 4.5 times higher than the most white tracts. Educational attainment is the only demographic variable considered in this study that exhibits a different relationship with primary road density, and we observe a U-shaped relationship between these variables (Figure 3).

To better understand the impact of the lockdowns on NO_2 exposure disparities, we consider case studies of individual cities: New York, Detroit, and Atlanta (Figure 4). Among individual neighborhoods in each of these cities, the magnitude of NO_2 drops vary up to 50% above and below the citywide average (Figure 4a-c). The portions of New York, Atlanta, and Detroit that received the largest drops tend to have lower median household income and a high percentage of non-white residents (Figure 4d-i). In New York the largest drops are concentrated in Harlem and The South Bronx (Figure 4a), where the high concentration of major highways and industrial facilities has been linked to disproportionate exposure to air pollution [Patel et al., 2009]. The largest drops in Atlanta occur in the southwestern part of the city where median household income generally is $<$ \$30000 and the percentage of Black residents in each tract is nearly 100. Although large-scale drops in NO_2 are primarily driven by reductions in on-road emissions [Quéré et al., 2020, Venter et al., 2020], examining drops on smaller spatial scales, such as in Atlanta (Figure 4b), suggests that emissions from other sectors may be at play. In Atlanta, the largest drops occur southwest of downtown, near Hartsfield-Jackson International Airport and several major highways (Figure 4b). The airport reported a $\sim 50\%$ decrease in the daily number of flights during lockdowns [Shah, 2020]. Therefore, both on-road and aviation emissions may be responsible for the disparities in NO_2 levels in Atlanta. The largest drops in Detroit are concentrated on the west shores of the Detroit River; Interstates 75 and 94 and the Ambassador Bridge, one of the busiest U.S.-Canada border crossing, transect this part of Detroit (Figure 4c) [Martenies et al., 2017]. Although these Detroit neighborhoods are not predominantly non-white (Figure 4f), they are home to a large Hispanic population (not shown) with low median household income (Figure 4i).

5. Discussion

Our results reveal that neighborhoods with a large population of racial and ethnic minorities, lower income, and lower educational attainment saw improvements in NO_2 pollution during the COVID-19 lockdowns. In many cases, though, NO_2 disparities during the baseline period were so large that disadvantaged communities faced higher NO_2 levels during the lockdowns than advantaged communities experienced prior to the lockdowns. Overall, these findings are consistent with contemporaneous studies that have analyzed long-term trends in NO_2 and other air pollutants and found that, despite widespread decreases in pollution, the most exposed demographic subgroups in the 1980s and 1990s remain the most exposed in the present-day [Clark et al., 2017, Colmer et al., 2020].

Disparities for certain spatial aggregations or for particular demographic variables deviate from the overall conclusions of this study. As an example, median household income is $\sim$ \$3000 higher in urban tracts with the largest drops compared with those with the smallest drops, which may be counterintuitive given the lower educational attainment (Figure 1e-f). Hajat et al. [Hajat et al., 2015] found higher concentrations of particulate matter and NO_x in neighborhoods with higher socioeconomic status in some North American cities. They posited that busy roadways often run along rivers and lakes, and higher socioeconomic status individuals may choose to live near these features for more scenic views and access to urban amenities. We also find higher baseline NO_2 for the most white and most educated tracts when considering all census tracts and only rural tracts (Figure 2b-c). A possible explanation for this may be that white, educated subpopulations choose to live in suburban areas outside the census-designed urban boundaries but within the polluted airshed of the city.

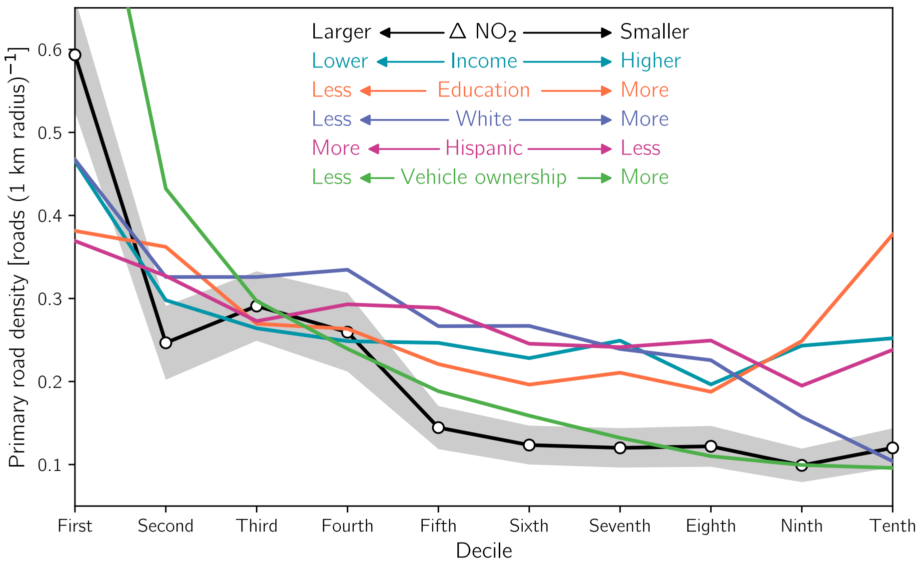

FIGURE 3. **The relationship of road density with urban lockdown-related drops in NO_2 columns and demographic variables.** Road density is calculated as the number of primary road segments within a 1 km radius of tracts' centroids for each decile of demographic variables. The colored legend indicates the directionality of each demographic variable. As an example, the density corresponding to the lowest decile of the "White" curve represents the road density in urban tracts that are the least white (i.e. in the first decile of the percentage of their population that is white). Shading for the ΔNO_2 curve indicates the 90% confidence interval.

Tracts' proximities to roadways may be responsible for both the lockdown-related drops and the persistent disparities of NO_2 pollution among demographic subgroups (Figures 1-3). The collocation of primary roads with poor, minority communities is not happenstance but a consequence of the Eisenhower-era federal highway program, which often deliberately routed highways through these poor, minority neighborhoods [Rose and Mohl, 2012, Boehmer et al., 2013, Rowangould, 2013, Clark et al., 2017]. Additionally, other potent sources of pollution such as power plants, manufacturing facilities, and heavy-duty trucking operations are also collocated with primary roads due to these industries' needs for highway access [Mohai et al., 2009, Demetillo et al., 2020].

Interestingly, urban tracts with the lowest vehicle ownership have both the highest density of nearby primary roads and the largest drops in NO_2 (Figures 1h, 3). This result suggests that these communities may breathe more traffic-related NO_2 pollution than they produce. This is indeed the case for particulate matter pollution: recent work found that particulate matter exposure is disproportionately caused by rich, non-Hispanic white communities, while poor, Black and Hispanic communities face higher exposure than is caused by their own consumption [Tessum et al., 2019, Sergi et al., 2020].

Preliminary research suggests that high levels of NO_2 pollution contribute to underlying health conditions that lead to increased COVID-19 fatality rates [Liang et al., 2020]. Therefore, the decrease in NO_2 in low income or ethnicity and racially diverse communities (Figure 2) could decrease population susceptibility to COVID-19. This is especially important as these communities have increased risk to COVID-19 and higher hospitalization rates [Raifman and Raifman, 2020]. Since short-term NO_2 exposure is associated with respiratory disease [Chauhan et al., 2003, Hansel et al., 2015], the temporary NO_2 drops may have reduced acute respiratory health outcomes, but the actual health effects of NO_2 drops during the pandemic are difficult to tease out since the degree to which people sought health care was also affected by the pandemic. These findings are especially relevant for disadvantaged neighborhoods in cities (e.g., New York, Atlanta, and Detroit; Figure 4) that have been long-plagued by high rates of asthma and other respiratory diseases due, in part, to their proximity to on-road and point source NO_x emissions [Patel et al., 2009, Martenies et al., 2017].

We have considered singular demographic variables and their relationship with baseline and lockdown NO_2. The case studies in Figure 4 hint that the intersectionality between race and poverty may be associated with even more pronounced lockdown-related drops in NO_2 pollution. Although the vast majority of tracts in the southern half of Atlanta have a majority non-white population (Figure 4h), the largest drops occur in tracts that are both majority non-white and low income (Figure 4b, e, h). Recent work by Demetillo et al. [Demetillo et al., 2020] examined NO_2 exposure for Houston neighborhoods where poverty and racial and ethnic identities intersect and found a disproportionate share of NO_2 pollution for neighborhoods with these intersecting identities. Assessing other forms of intersectionality and their relationship with air pollution exposure is a key area for future research.

We relied on TROPOMI tropospheric column abundances rather than surface-level concentrations to understand the impact of lockdowns on disparities in NO_2. Surface-level NO_2 concentrations inferred from satellites exist [Geddes et al., 2016, Cooper et al., 2020], but not for 2020. Surface-level observations are sparse and unevenly distributed in the U.S. [Lamsal et al., 2015]. TROPOMI provides significant advances over predecessor instruments on account of its unprecedented

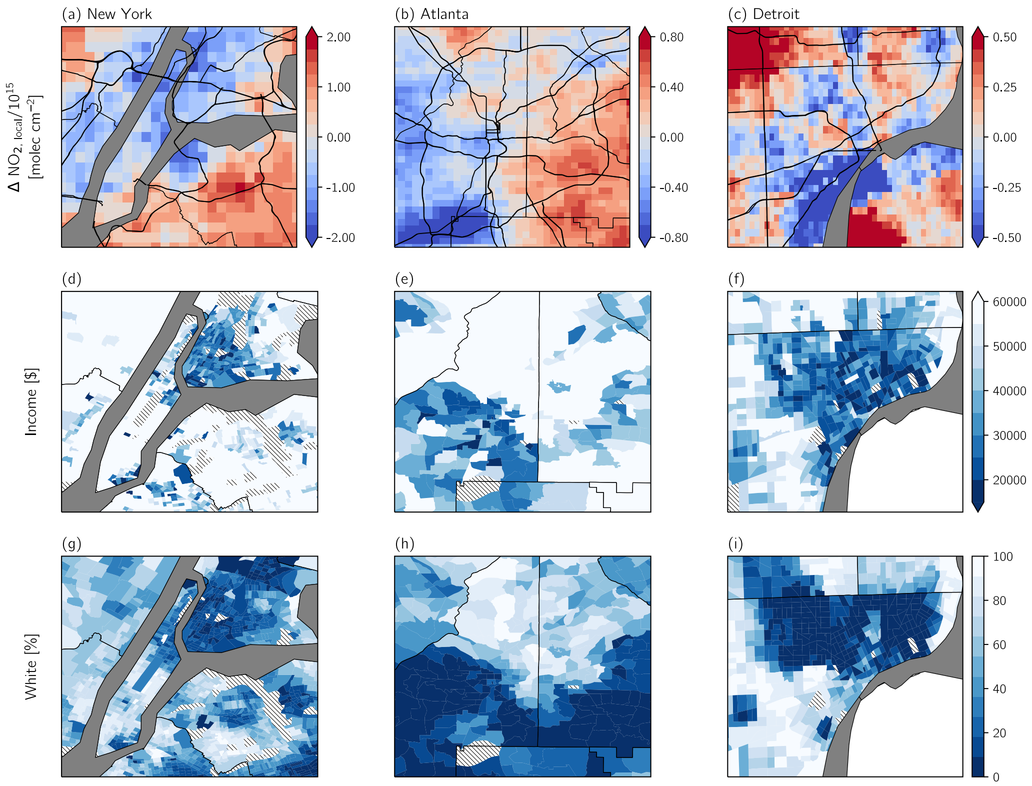

FIGURE 4. **Case studies of lockdown NO_2 drops, income, and race for (left column) New York, (middle) Atlanta, and (right) Detroit.** (a-c) Δ $NO_{2,\,\mathrm{local}}$ is calculated from oversampled TROPOMI data as the difference between Δ NO_2 and the city average Δ NO_2 to highlight neighborhoods with larger drops (i.e., negative values) and smaller drops (i.e., positive values) compared with the city-averaged drops. Primary roads are shown in thick black lines. (d-f) Median household income and (g-i) percentage of the population that is white. Tracts in (d-i) that are employment centers, airports, parks, or forests and therefore report no demographic data are denoted with hatching.

spatial resolution [Goldberg et al., 2019] and has been used for understanding ethnic, racial, and socioeconomic status NO_2 disparities [Demetillo et al., 2020]. We tested whether TROPOMI has consistent spatial patterns with surface-level observations and found good agreement (Figure S4a, Supporting Information Text). The ratios of 24-hour average NO_2 to NO_2 near the time of satellite overpass are also similar between least- and most-polluted sites (Figure S4b). These results suggest that column-to-surface or time-to-day biases do not underscore TROPOMI's ability to capture disparities. Future work may infer surface concentrations of NO_2 from satellite-derived column abundances during lockdowns using these satellite data within land-use regression models [Novotny et al., 2011] or chemical transport models [Cooper et al., 2020]. We encourage the use of these ground-level estimates to better understand exposure across demographic subgroups.

Lockdown-related changes in other air pollutants, particularly secondary pollutants such as ozone and particulate matter, do not exhibit the same spatial patterns as NO_2 [Chang et al., 2020, Shi and Brasseur, 2020, Venter et al., 2020]. Future research should investigate how changes in these species impact pollutant disparities and environmental justice during lockdowns.

6. Conclusions

This study provides a unique look at air pollution disparities in the U.S., leveraging the extraordinary confluence of unparalleled changes in human activity during COVID-19 lockdowns and unmatched spatial coverage and resolution of air quality surveillance from the TROPOMI satellite instrument. Lockdowns decreased tropospheric column abundances of NO_2 across the vast majority of urban areas. However, drops in NO_2 pollution were uneven within these urban areas and largely benefitted communities with a high proportion of racial and ethnic minorities and lower educational attainment. Our results reveal that, despite the improvements in NO_2 pollution during lockdowns, minority communities and communities with lower income and educational attainment continued to face higher levels of NO_2 during the lockdowns than majority white communities and those with higher income and educational attainment experienced prior to the pandemic. As traffic emissions represent a major source of NO_2 variability, the proximity of disadvantaged neighborhoods to a high density of major roadways is likely the key determinant in explaining lockdown-related drops in NO_2 pollution.

Our finding that even the $\sim 50\%$ drop in passenger vehicle emissions [Quéré et al., 2020] did not reduce NO_2 levels among the most disadvantaged urban census tracts to the levels experienced by the most advantaged tracts before the pandemic indicates that profound changes are needed to address disparities in NO_2 pollution in the U.S. In particular, this unintended natural experiment shows that policies aimed at reducing emissions from passenger vehicle traffic (e.g., mode shifting to public transportation and active transportation, widespread use of electric vehicles) would not be enough. Policy strategies such as traffic rerouting and low emissions zones [Nguyen and Marshall, 2018] and the widespread electrification of heavy-, medium- and light-duty vehicles [Peters et al., 2020] are urgently needed. Moreover, as stationary sources (e.g., power plants, industrial facilities) are often collocated with major highways and interstates, emission control strategies that reduce inequality in exposure while maximizing health benefits [Levy et al., 2007] from these stationary sources should also be a key priority.

7. Materials and Methods

7.1. **Remotely-sensed NO_2.** We obtain retrievals of the tropospheric NO_2 column from the Tropospheric Monitoring Instrument (TROPOMI) aboard the Sentinel-5 Precursor (S5P) satellite. S5P is a nadir-viewing satellite in a sun-synchronous, low-earth orbit that achieves near-global daily coverage with a local overpass time of $\sim$ 1330 hours [Veefkind et al., 2012]. TROPOMI provides NO_2 measurements at an unprecedented spatial resolution of 5×3.5 km^2 (7×3.5 km^2 prior to 6 August 2019) [van Geffen et al., 2020]. Specifically, we use Level 2 data and only consider pixels with a quality assurance value > 0.75. Data are thereafter oversampled by regridding to a standard grid with a resolution of 0.01° latitude $\times$ 0.01° longitude ($\sim$ 1 km $\times$1 km) and averaged over two time periods: a baseline period (13 March-13 June 2019) and a lockdown period (13 March-13 June 2020). Regridded data are publicly available at Figshare (`www.figshare.com/s/75a00608f3faedc4bca7`).

Comparing the same time period across different years is commonplace in satellite studies investigating changes in NO_x and other trace gases, and averaging over three month timeframes smooths natural NO_2 variations that arise from differences in meteorology and sun angle, which are especially relevant during boreal spring [Goldberg et al., 2020b]. This temporal averaging also removes part of the random error in the TROPOMI single-pixel uncertainties, which can be 40-60% of the tropospheric column abundances [Bauwens et al., 2020].

7.2. **Socio-demographic Data.** Demographic information is derived from the American Community Survey (ACS) conducted by the U.S. Census Bureau and maintained by the National Historical Geographic Information System [Manson et al., 2019]. Data are publicly available at `www.nhgis.org`. We extract 2014-2018 5-year estimates on race, Hispanic or Latino origin (henceforth "ethnicity"), educational attainment, median household income, and vehicle availability for the 72,538 census tracts in the contiguous U.S. To minimize the number of different categorical variables presented in this study, we combine racial groups into three categories: white, Black (includes Black and African American), and Other (includes American Indian/Alaska Native, Asian, Native Hawaiian/Other Pacific Islander, and some other race). Similarly, we form three different levels for educational attainment: high school (includes no high school diploma, regular high school diploma, and GED or alternative credentials), college (includes some college without a degree, Associate's degree, and Bachelor's degree), and graduate (includes Master's degree, Professional school degree, and Doctorate degree).

7.3. **Methods.** We harmonize the regridded TROPOMI NO_2 measurements with tract-level ACS demographics by determining the geographic boundaries of each tract and thereafter calculating a simple arithmetic average over all TROPOMI grid cells within the tract for the baseline and lockdown periods. Approximately 8% of tracts lack a co-located TROPOMI grid cell due to their small size or irregular geometry, and we exclude these tracts from our analysis. Tracts are classified as either rural or urban based on the census-designed rurality level from the last decadal census in 2010. We further stratify the tracts into metropolitan-level subsets for the 15 largest metropolitan statistical areas (MSAs) in the U.S.: New York City-Newark-Jersey City, NY-NJ-PA; Los Angeles-Long Beach-Anaheim, CA; Chicago-Naperville-Elgin, IL-IN-WI; Dallas-Fort Worth-Arlington, TX; Houston-The Woodlands-Sugar Land, TX; Washington-Arlington-Alexandria, DC-VA-MD-WV; Miami-Fort Lauderdale-Pompano Beach, FL; Philadelphia-Camden-Wilmington, PA-NJ-DE-MD; Atlanta-Sandy Springs-Alpharetta, GA; Phoenix-Mesa-Chandler, AZ; Boston-Cambridge-Newton, MA-NH; San Francisco-Oakland-Berkeley, CA; Riverside-San Bernardino-Ontario, CA; Detroit-Warren-Dearborn, MI; and Seattle-Tacoma-Bellevue, WA. For brevity we refer to these MSAs by their colloquial names (e.g., Los Angeles, rather than Los Angeles-Long Beach-Anaheim, CA) when discussing them.

We calculate the density of nearby primary roadways for each census tract as a proxy for exposure to traffic-related NO_2 pollution. Primary roads are generally divided, limited-access highways within the Interstate Highway System or under state management, and their locations are determined from the U.S. Census Bureau's TIGER/Line geospatial database. Specifically, we determine density as the number of primary road segments within 1 km of a tract's centroid. We choose 1 km as our threshold for what constitutes as "nearby," as NO_2 concentrations decrease up to $\sim 50\%$ within $0.5 - 2$ km from major roadways [Novotny et al., 2011, Demetillo et al., 2020], and we note that our findings are robust when considering all primary roads within 2 km (not shown). Other means of quantifying traffic exist (e.g., length of roadway within a specified distance, traffic within buffer zones, sum of distance traveled) [Pratt et al., 2013], but our approach allows for consistent use of geospatial data from the U.S. Census Bureau.

We partition census tracts by extreme values of their change in NO_2 (Δ NO_2) or demographic variables using the first decile (0-10th percentile) and tenth decile (90-100th percentile). As examples, tracts classified as "Most white" or "Highest income" have a white population fraction or median household income which falls in the tenth decile. Likewise, Δ NO_2 in tracts with the "Largest drops" (i.e., the largest decrease in NO_2 during lockdowns) falls in the first decile. Our results are not sensitive to the use of the first and tenth deciles, and we have tested the upper and lower vigintiles, quintiles, and quartiles and obtain similar results (Figure S2). The use of percentiles rather than absolute thresholds yields a consistent sample size for the upper and lower extrema and also avoids defining absolute thresholds for different variables. This is especially important as thresholds may change along the urban-rural gradient or among different metropolitan areas.

The start date of the baseline and lockdowns periods used in this study (13 March) corresponds to the date of national emergency declaration in the U.S. and the beginning of a pronounced decrease in mobility patterns in 2020 [Badr et al., 2020]. Our results could be an artifact of the start date or length of the baseline and lockdown periods. We test whether the overall racial, ethnic, income, and educational disparities hold for other periods and find that the disparities among different demographic subgroups persist regardless of the start date or length of the baseline period (Figure S3). While the absolute NO_2 levels experienced by these subgroups slightly change based on the baseline period, our overall results do not hinge on the precise definition of the baseline period. We are inherently limited by the short TROPOMI data record, and interannual variability could play a role in modulating the magnitude of disparities in NO_2 levels. Testing this possibility is important as more TROPOMI data become available.

8. Acknowledgement

Research reported in the publication was supported by NASA under award numbers 80NSSC19K0193 and 80NSSC20K1122. Regridded TROPOMI data used in this study are freely available on Figshare (`www.figshare.com/s/75a00608f3faedc4bca7`), and ACS demographic data are available at `www.nhgis.org`. The authors would like to thank the Netherlands Space Office and European Space Agency for their support of TROPOMI products.

References

[Achakulwisut et al., 2019] Achakulwisut, P., Brauer, M., Hystad, P., and Anenberg, S. C. (2019). Global, national, and urban burdens of paediatric asthma incidence attributable to ambient NO_2 pollution: estimates from global datasets. *The Lancet Planetary Health*, 3(4):e166–e178.

[Anenberg et al., 2018] Anenberg, S. C., Henze, D. K., Tinney, V., Kinney, P. L., Raich, W., Fann, N., Malley, C. S., Roman, H., Lamsal, L., Duncan, B., Martin, R. V., van Donkelaar, A., Brauer, M., Doherty, R., Jonson, J. E., Davila, Y., Sudo, K., and Kuylenstierna, J. C. (2018). Estimates of the global burden of ambient $PM_{2.5}$, ozone, and NO_2 on asthma incidence and emergency room visits. *Environmental Health Perspectives*, 126(10):107004.

[Badr et al., 2020] Badr, H. S., Du, H., Marshall, M., Dong, E., Squire, M. M., and Gardner, L. M. (2020). Association between mobility patterns and COVID-19 transmission in the USA: a mathematical modelling study. *The Lancet Infectious Diseases*.

[Bauwens et al., 2020] Bauwens, M., Compernolle, S., Stavrakou, T., Müller, J.-F., Gent, J., Eskes, H., Levelt, P. F., A, R., Veefkind, J. P., Vlietinck, J., Yu, H., and Zehner, C. (2020). Impact of coronavirus outbreak on NO_2 pollution assessed using TROPOMI and OMI observations. *Geophysical Research Letters*, 47(11).

[Bell and Ebisu, 2012] Bell, M. L. and Ebisu, K. (2012). Environmental inequality in exposures to airborne particulate matter components in the United States. *Environmental Health Perspectives*, 120(12):1699–1704.

[Boehmer et al., 2013] Boehmer, T. K., Foster, S. L., Henry, J. R., Woghiren-Akinnifesi, E. L., and Yip, F. Y. (2013). Residential proximity to major highways - United States, 2010. *Morbidity and Mortality Weekly Report*, 62(3):46–50.

[Chang et al., 2020] Chang, Y., Huang, R.-J., Ge, X., Huang, X., Hu, J., Duan, Y., Zou, Z., Liu, X., and Lehmann, M. F. (2020). Puzzling haze events in china during the coronavirus (COVID-19) shutdown. *Geophysical Research Letters*, 47(12).

[Chauhan et al., 2003] Chauhan, A., Inskip, H. M., Linaker, C. H., Smith, S., Schreiber, J., Johnston, S. L., and Holgate, S. T. (2003). Personal exposure to nitrogen dioxide (NO_2) and the severity of virus-induced asthma in children. *The Lancet*, 361(9373):1939–1944.

[Clark et al., 2014] Clark, L. P., Millet, D. B., and Marshall, J. D. (2014). National patterns in environmental injustice and inequality: Outdoor NO_2 air pollution in the united states. *PLoS ONE*, 9(4):e94431.

[Clark et al., 2017] Clark, L. P., Millet, D. B., and Marshall, J. D. (2017). Changes in transportation-related air pollution exposures by race-ethnicity and socioeconomic status: outdoor nitrogen dioxide in the United States in 2000 and 2010. *Environmental Health Perspectives*, 125(9):097012.

[Colmer et al., 2020] Colmer, J., Hardman, I., Shimshack, J., and Voorheis, J. (2020). Disparities in $PM_{2.5}$ air pollution in the United States. *Science*, 369(6503):575–578.

[Cooper et al., 2020] Cooper, M. J., Martin, R. V., McLinden, C. A., and Brook, J. R. (2020). Inferring ground-level nitrogen dioxide concentrations at fine spatial resolution applied to the TROPOMI satellite instrument. *Environmental Research Letters*, 15(10):104013.

[Demetillo et al., 2020] Demetillo, M. A. G., Navarro, A., Knowles, K. K., Fields, K. P., Geddes, J. A., Nowlan, C. R., Janz, S. J., Judd, L. M., Al-Saadi, J., Sun, K., McDonald, B. C., Diskin, G. S., and Pusede, S. E. (2020). Observing nitrogen dioxide air pollution inequality using high-spatial-resolution remote sensing measurements in houston, texas. *Environmental Science & Technology*, 54(16):9882–9895.

[Diffenbaugh et al., 2020] Diffenbaugh, N. S., Field, C. B., Appel, E. A., Azevedo, I. L., Baldocchi, D. D., Burke, M., Burney, J. A., Ciais, P., Davis, S. J., Fiore, A. M., Fletcher, S. M., Hertel, T. W., Horton, D. E., Hsiang, S. M., Jackson, R. B., Jin, X., Levi, M., Lobell, D. B., McKinley, G. A., Moore, F. C., Montgomery, A., Nadeau, K. C., Pataki, D. E., Randerson, J. T., Reichstein, M., Schnell, J. L., Seneviratne, S. I., Singh, D., Steiner, A. L., and Wong-Parodi, G. (2020). The COVID-19 lockdowns: a window into the earth system. *Nature Reviews Earth & Environment*, 1(9):470–481.

[Geddes et al., 2016] Geddes, J. A., Martin, R. V., Boys, B. L., and van Donkelaar, A. (2016). Long-term trends worldwide in ambient NO_2 concentrations inferred from satellite observations. *Environmental Health Perspectives*, 124(3):281–289.

[Goldberg et al., 2020a] Goldberg, D. L., Anenberg, S., Mohegh, A., Lu, Z., and Streets, D. G. (2020a). TROPOMI NO_2 in the United States: a detailed look at the annual averages, weekly cycles, effects of temperature, and correlation with $PM_{2.5}$. *Unpublished results*.

[Goldberg et al., 2020b] Goldberg, D. L., Anenberg, S. C., Griffin, D., McLinden, C. A., Lu, Z., and Streets, D. G. (2020b). Disentangling the impact of the COVID-19 lockdowns on urban NO_2 from natural variability. *Geophysical Research Letters*, 47(17).

[Goldberg et al., 2019] Goldberg, D. L., Lu, Z., Streets, D. G., de Foy, B., Griffin, D., McLinden, C. A., Lamsal, L. N., Krotkov, N. A., and Eskes, H. (2019). Enhanced capabilities of TROPOMI NO_2: Estimating NO_x from North American cities and power plants. *Environmental Science & Technology*, 53(21):12594–12601.

[Hajat et al., 2013] Hajat, A., Diez-Roux, A. V., Adar, S. D., Auchincloss, A. H., Lovasi, G. S., O'Neill, M. S., Sheppard, L., and Kaufman, J. D. (2013). Air pollution and individual and neighborhood socioeconomic status: Evidence from the multi-ethnic study of atherosclerosis (MESA). *Environmental Health Perspectives*, 121(11-12):1325–1333.

[Hajat et al., 2015] Hajat, A., Hsia, C., and O'Neill, M. S. (2015). Socioeconomic disparities and air pollution exposure: a global review. *Current Environmental Health Reports*, 2(4):440–450.

[Hansel et al., 2015] Hansel, N. N., McCormack, M. C., and Kim, V. (2015). The effects of air pollution and temperature on COPD. *COPD: Journal of Chronic Obstructive Pulmonary Disease*, 13(3):372–379.

[He et al., 2020] He, G., Pan, Y., and Tanaka, T. (2020). The short-term impacts of COVID-19 lockdown on urban air pollution in China. *Nature Sustainability*.

[Jerrett et al., 2013] Jerrett, M., Burnett, R. T., Beckerman, B. S., Turner, M. C., Krewski, D., Thurston, G., Martin, R. V., van Donkelaar, A., Hughes, E., Shi, Y., Gapstur, S. M., Thun, M. J., and Pope, C. A. (2013). Spatial analysis of air pollution and mortality in California. *American Journal of Respiratory and Critical Care Medicine*, 188(5):593–599.

[Krotkov et al., 2017] Krotkov, N. A., Lamsal, L. N., Celarier, E. A., Swartz, W. H., Marchenko, S. V., Bucsela, E. J., Chan, K. L., Wenig, M., and Zara, M. (2017). The version 3 OMI no_2 standard product. *Atmospheric Measurement Techniques*, 10(9):3133–3149.

[Lamsal et al., 2015] Lamsal, L. N., Duncan, B. N., Yoshida, Y., Krotkov, N. A., Pickering, K. E., Streets, D. G., and Lu, Z. (2015). U.S. NO_2 trends (2005-2013): EPA Air Quality System (AQS) data versus improved observations from the Ozone Monitoring Instrument (OMI). *Atmospheric Environment*, 110:130–143.

[Landrigan et al., 2018] Landrigan, P. J., Fuller, R., Acosta, N. J. R., Adeyi, O., Arnold, R., Basu, N. N., Baldé, A. B., Bertollini, R., Bose-O'Reilly, S., Boufford, J. I., Breysse, P. N., Chiles, T., Mahidol, C., Coll-Seck, A. M., Cropper, M. L., Fobil, J., Fuster, V., Greenstone, M., Haines, A., Hanrahan, D., Hunter, D., Khare, M., Krupnick, A., Lanphear, B., Lohani, B., Martin, K., Mathiasen, K. V., McTeer, M. A., Murray, C. J. L., Ndahimananjara, J. D., Perera, F., Potočnik, J., Preker, A. S., Ramesh, J., Rockström, J., Salinas, C., Samson, L. D., Sandilya, K., Sly, P. D., Smith, K. R., Steiner, A., Stewart, R. B., Suk, W. A., van Schayck, O. C. P., Yadama, G. N., Yumkella, K., and Zhong, M. (2018). The Lancet Commission on pollution and health. *The Lancet*, 391(10119):462–512.

[Lecocq et al., 2020] Lecocq, T., Hicks, S. P., Noten, K. V., van Wijk, K., Koelemeijer, P., Plaen, R. S. M. D., Massin, F., Hillers, G., Anthony, R. E., Apoloner, M.-T., Arroyo-Solórzano, M., Assink, J. D., Büyükakpınar, P., Cannata, A., Cannavo, F., Carrasco, S., Caudron, C., Chaves, E. J., Cornwell, D. G., Craig, D., den Ouden, O. F. C., Diaz, J., Donner, S., Evangelidis, C. P., Evers, L., Fauville, B., Fernandez, G. A., Giannopoulos, D., Gibbons, S. J., Girona, T., Grecu, B., Grunberg, M., Hetényi, G., Horleston, A., Inza, A., Irving, J. C. E., Jamalreyhani, M., Kafka, A., Koymans, M. R., Labedz, C. R., Larose, E., Lindsey, N. J., McKinnon, M., Megies, T., Miller, M. S., Minarik, W., Moresi, L., Márquez-Ramírez, V. H., Möllhoff, M., Nesbitt, I. M., Niyogi, S., Ojeda, J., Oth, A., Proud, S., Pulli, J., Retailleau, L., Rintamäki, A. E., Satriano, C., Savage, M. K., Shani-Kadmiel, S., Sleeman, R., Sokos, E., Stammler, K., Stott, A. E., Subedi, S., Sorensen, M. B., Taira, T., Tapia, M., Turhan, F., van der Pluijm, B., Vanstone, M., Vergne, J., Vuorinen, T. A. T., Warren, T., Wassermann, J., and Xiao, H. (2020). Global quieting of high-frequency seismic noise due to COVID-19 pandemic lockdown measures. *Science*, 369(6509):1338–1343.

[Levy et al., 2014] Levy, I., Mihele, C., Lu, G., Narayan, J., and Brook, J. R. (2014). Evaluating multipollutant exposure and urban air quality: pollutant interrelationships, neighborhood variability, and nitrogen dioxide as a proxy pollutant. *Environmental Health Perspectives*, 122(1):65–72.

[Levy et al., 2007] Levy, J. I., Wilson, A. M., and Zwack, L. M. (2007). Quantifying the efficiency and equity implications of power plant air pollution control strategies in the United States. *Environmental Health Perspectives*, 115(5):743–750.

[Liang et al., 2020] Liang, D., Shi, L., Zhao, J., Liu, P., Sarnat, J. A., Gao, S., Schwartz, J., Liu, Y., Ebelt, S. T., Scovronick, N., and Chang, H. H. (2020). Urban air pollution may enhance COVID-19 case-fatality and mortality rates in the united states. *The Innovation*, 1(3):100047.

[Manson et al., 2019] Manson, S., Schroeder, J., Riper, D. V., and Ruggles, S. (2019). National historical geographic information system: Version 14.0.

[Martenies et al., 2017] Martenies, S., Milando, C., Williams, G., and Batterman, S. (2017). Disease and health inequalities attributable to air pollutant exposure in detroit, michigan. *International Journal of Environmental Research and Public Health*, 14(10):1243.

[Mohai et al., 2009] Mohai, P., Lantz, P. M., Morenoff, J., House, J. S., and Mero, R. P. (2009). Racial and socioeconomic disparities in residential proximity to polluting industrial facilities: Evidence from the americans changing lives study. *American Journal of Public Health*, 99(S3):S649–S656.

[Nguyen and Marshall, 2018] Nguyen, N. P. and Marshall, J. D. (2018). Impact, efficiency, inequality, and injustice of urban air pollution: variability by emission location. *Environmental Research Letters*, 13(2):024002.

[Novotny et al., 2011] Novotny, E. V., Bechle, M. J., Millet, D. B., and Marshall, J. D. (2011). National satellite-based land-use regression: NO_2 in the united states. *Environmental Science & Technology*, 45(10):4407–4414.

[Patel et al., 2009] Patel, M. M., Chillrud, S. N., Correa, J. C., Feinberg, M., Hazi, Y., Deepti, K., Prakash, S., Ross, J. M., Levy, D., and Kinney, P. L. (2009). Spatial and temporal variations in traffic-related particulate matter at new york city high schools. *Atmospheric Environment*, 43(32):4975–4981.

[Peters et al., 2020] Peters, D. R., Schnell, J. L., Kinney, P. L., Naik, V., and Horton, D. E. (2020). Public health and climate benefits and trade-offs of U.S. vehicle electrification. *GeoHealth*, 4(10).

[Pratt et al., 2013] Pratt, G. C., Parson, K., Shinoda, N., Lindgren, P., Dunlap, S., Yawn, B., Wollan, P., and Johnson, J. (2013). Quantifying traffic exposure. *Journal of Exposure Science & Environmental Epidemiology*, 24(3):290–296.

[Quéré et al., 2020] Quéré, C. L., Jackson, R. B., Jones, M. W., Smith, A. J. P., Abernethy, S., Andrew, R. M., De-Gol, A. J., Willis, D. R., Shan, Y., Canadell, J. G., Friedlingstein, P., Creutzig, F., and Peters, G. P. (2020). Temporary reduction in daily global CO_2 emissions during the COVID-19 forced confinement. *Nature Climate Change*, 10(7):647–653.

[Raifman and Raifman, 2020] Raifman, M. A. and Raifman, J. R. (2020). Disparities in the population at risk of severe illness from COVID-19 by race/ethnicity and income. *American Journal of Preventive Medicine*, 59(1):137–139.

[Rose and Mohl, 2012] Rose, M. H. and Mohl, R. A. (2012). *Interstate: Highway Politics and Policy since 1939.* The University of Tennessee Press, Knoxville, 3rd edition.

[Rowangould, 2013] Rowangould, G. M. (2013). A census of the US near-roadway population: Public health and environmental justice considerations. *Transportation Research Part D: Transport and Environment*, 25:59–67.

[Schell et al., 2020] Schell, C. J., Dyson, K., Fuentes, T. L., Roches, S. D., Harris, N. C., Miller, D. S., Woelfle-Erskine, C. A., and Lambert, M. R. (2020). The ecological and evolutionary consequences of systemic racism in urban environments. *Science*, 369(6510):eaay4497.

[Sergi et al., 2020] Sergi, B., Azevedo, I., Davis, S. J., and Muller, N. Z. (2020). Regional and county flows of particulate matter damage in the US. *Environmental Research Letters*, 15(10):104073.

[Shah, 2020] Shah, K. (2020). 'Mostly empty': Covid-19 has nearly shut down world's busiest airport. Accessed October 15, 2020.

[Shi and Brasseur, 2020] Shi, X. and Brasseur, G. P. (2020). The response in air quality to the reduction of Chinese economic activities during the COVID-19 outbreak. *Geophysical Research Letters*, 47(11).

[Stohl et al., 2015] Stohl, A., Aamaas, B., Amann, M., Baker, L. H., Bellouin, N., Berntsen, T. K., Boucher, O., Cherian, R., Collins, W., Daskalakis, N., Dusinska, M., Eckhardt, S., Fuglestvedt, J. S., Harju, M., Heyes, C., Hodnebrog, Ø., Hao, J., Im, U., Kanakidou, M., Klimont, Z., Kupiainen, K., Law, K. S., Lund, M. T., Maas, R., MacIntosh, C. R., Myhre, G., Myriokefalitakis, S., Olivié, D., Quaas, J., Quennehen, B., Raut, J.-C., Rumbold, S. T., Samset, B. H., Schulz, M., Seland, Ø., Shine, K. P., Skeie, R. B., Wang, S., Yttri, K. E., and Zhu, T. (2015). Evaluating the climate and air quality impacts of short-lived pollutants. *Atmospheric Chemistry and Physics*, 15(18):10529–10566.

[Sundvor et al., 2013] Sundvor, I., Balaguer, N. C., Viana, M., Querol, X., Reche, C., Amato, F., Mellios, G., and Guerreiro, C. (2013). Road traffic's contribution to air quality in European cities. Technical report, European Topic Centre for Air Pollution and Climate Change Mitigation.

[Tessum et al., 2019] Tessum, C. W., Apte, J. S., Goodkind, A. L., Muller, N. Z., Mullins, K. A., Paolella, D. A., Polasky, S., Springer, N. P., Thakrar, S. K., Marshall, J. D., and Hill, J. D. (2019). Inequity in consumption of goods and services adds to racial–ethnic disparities in air pollution exposure. *Proceedings of the National Academy of Sciences*, 116(13):6001–6006.

[US Environmental Protection Agency, 2015] US Environmental Protection Agency (2015). 2014 National Emissions Inventory (NEI) data. `https://www.epa.gov/air-emissions-inventories/2014-national-emissions-inventory-nei-data`. Accessed October 15, 2020.

[van Geffen et al., 2020] van Geffen, J., Boersma, K. F., Eskes, H., Sneep, M., ter Linden, M., Zara, M., and Veefkind, J. P. (2020). S5P TROPOMI NO_2 slant column retrieval: method, stability, uncertainties and comparisons with OMI. *Atmospheric Measurement Techniques*, 13(3):1315–1335.

[Veefkind et al., 2012] Veefkind, J., Aben, I., McMullan, K., Förster, H., de Vries, J., Otter, G., Claas, J., Eskes, H., de Haan, J., Kleipool, Q., van Weele, M., Hasekamp, O., Hoogeveen, R., Landgraf, J., Snel, R., Tol, P., Ingmann, P., Voors, R., Kruizinga, B., Vink, R., Visser, H., and Levelt, P. (2012). TROPOMI on the ESA Sentinel-5 Precursor: a GMES mission for global observations of the atmospheric composition for climate, air quality and ozone layer applications. *Remote Sensing of Environment*, 120:70–83.

[Venter et al., 2020] Venter, Z. S., Aunan, K., Chowdhury, S., and Lelieveld, J. (2020). COVID-19 lockdowns cause global air pollution declines. *Proceedings of the National Academy of Sciences*, 117(32):18984–18990.

SUPPORTING INFORMATION FOR "COVID-19 LOCKDOWNS REVEAL PRONOUNCED DISPARITIES IN NITROGEN DIOXIDE POLLUTION LEVELS"

GAIGE HUNTER KERR[1], DANIEL L. GOLDBERG[1,2], SUSAN C. ANENBERG[1]

[1] *Department of Environmental and Occupational Health, Milken Institute School of Public Health, George Washington University, Washington, DC, 20052 USA,*
[2] *Energy Systems Division, Argonne National Laboratory, Lemont, IL, 60439 USA*

1. Remotely-sensed versus surface-level NO_2

We compare tropospheric column NO_2 from TROPOMI with ground-based observations from the Environmental Protection Agency's Air Quality System (AQS) [US Environmental Protection Agency, nda] to test whether TROPOMI can provide an accurate characterization of differences in surface-level NO_2. There are 439 AQS monitors in the contiguous U.S. with observations during the baseline period, and we average hourly observations over the entire baseline period at each of these sites and compare it with TROPOMI retrievals at the collocated grid cell to each site.

TROPOMI struggles to capture large, localized sources of NO_2 on account of the difference in scale between the footprint of the satellite and point-based observations [Judd et al., 2019]. We find that 71 of the 439 monitors are located near ($<$ 20 meters) roads [US Environmental Protection Agency, ndb]. These sites generally have observed surface-level $NO_2 > 10$ ppbv despite relatively low columnar amounts from TROPOMI (Figure 4). When we consider only AQS monitors that are not located near roads, we find good agreement between TROPOMI and AQS NO_2 levels (Figure 4a). We also find a similar ratio of NO_2 averaged over the 24-hour diurnal cycle to NO_2 near the time of satellite overpass at sites that are classified as the most and least polluted (Figure 4b). These findings lend credibility to our reliance on TROPOMI to characterize disparities in NO_2 at earth's surface.

E-mail address: gaigekerr@gwu.edu.

References

[Judd et al., 2019] Judd, L. M., Al-Saadi, J. A., Janz, S. J., Kowalewski, M. G., Pierce, R. B., Szykman, J. J., Valin, L. C., Swap, R., Cede, A., Mueller, M., Tiefengraber, M., Abuhassan, N., and Williams, D. (2019). Evaluating the impact of spatial resolution on tropospheric NO_2 column comparisons within urban areas using high-resolution airborne data. *Atmospheric Measurement Techniques*, 12(11):6091–6111.

[US Environmental Protection Agency, nda] US Environmental Protection Agency (n.d.a). Air Quality System Data Mart. `https://www.epa.gov/airdata`. Accessed October 21, 2020.

[US Environmental Protection Agency, ndb] US Environmental Protection Agency (n.d.b). Near-road NO_2 monitoring. `https://www3.epa.gov/ttnamti1/nearroad.html`. Accessed October 22, 2020.

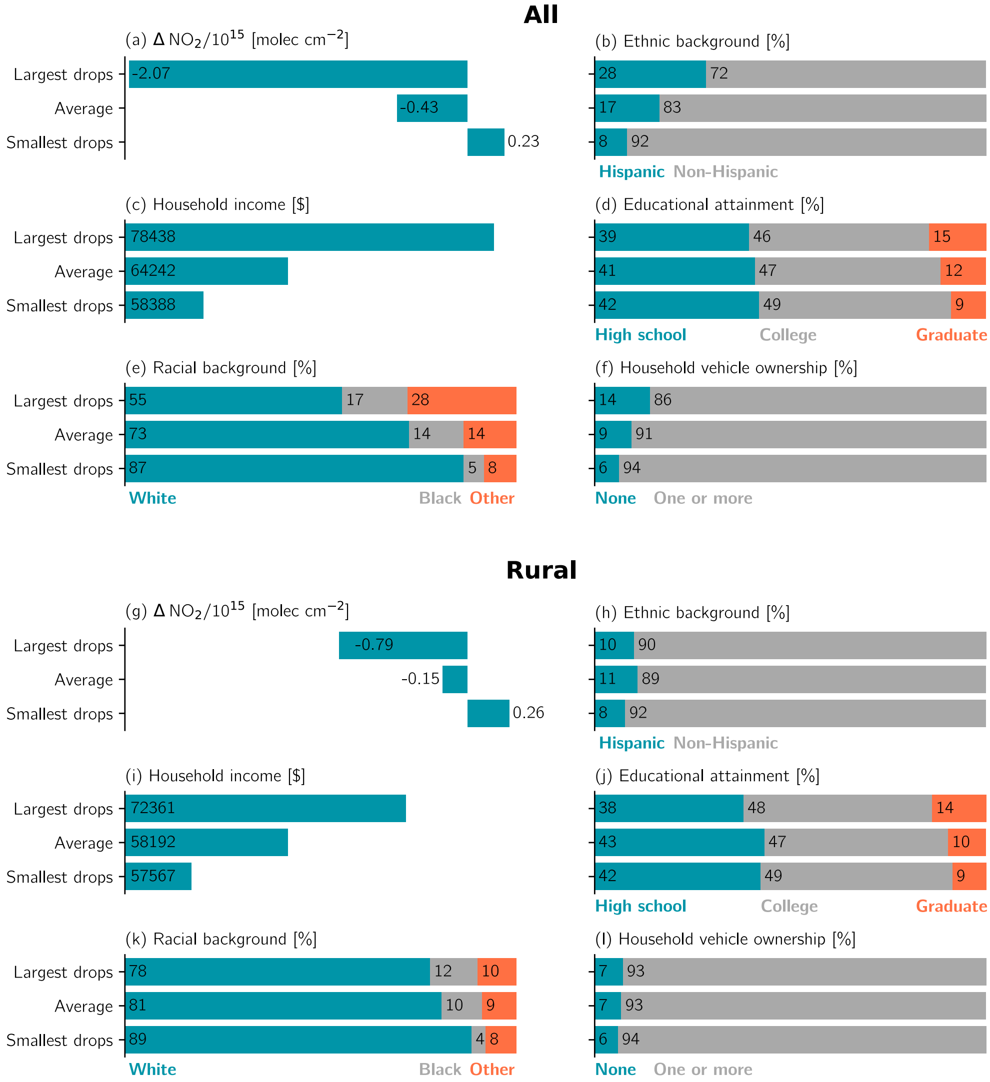

FIGURE 1. Same as Figure 1c-h in the main text but drops and averages are derived from (a-f) all tracts and (g-l) rural tracts.

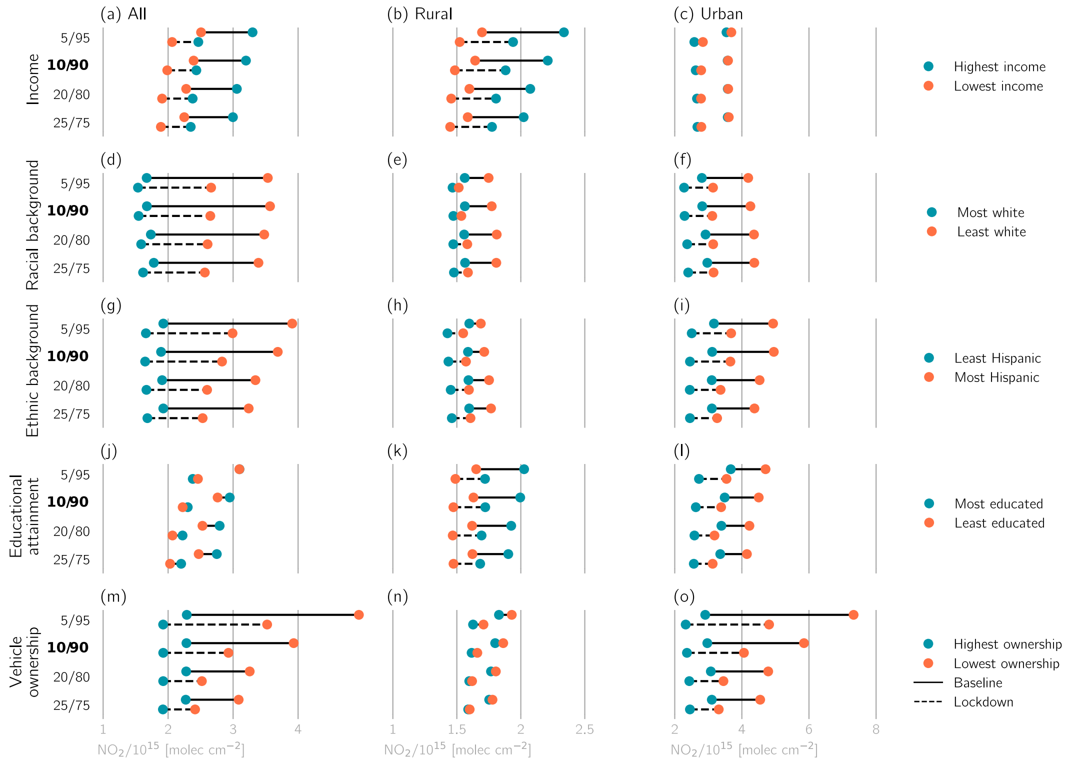

FIGURE 2. **Sensitivity of NO_2 disparities to percentiles chosen to constitute extreme values for each demographic variable.** Interpretation follows Figure 2 in the main text, but each pair of bars in individual subplots represents different percentile thresholds, indicated in the subplots' vertical axes. The boldface 10/90 row corresponds to the first and tenth deciles used in the main text.

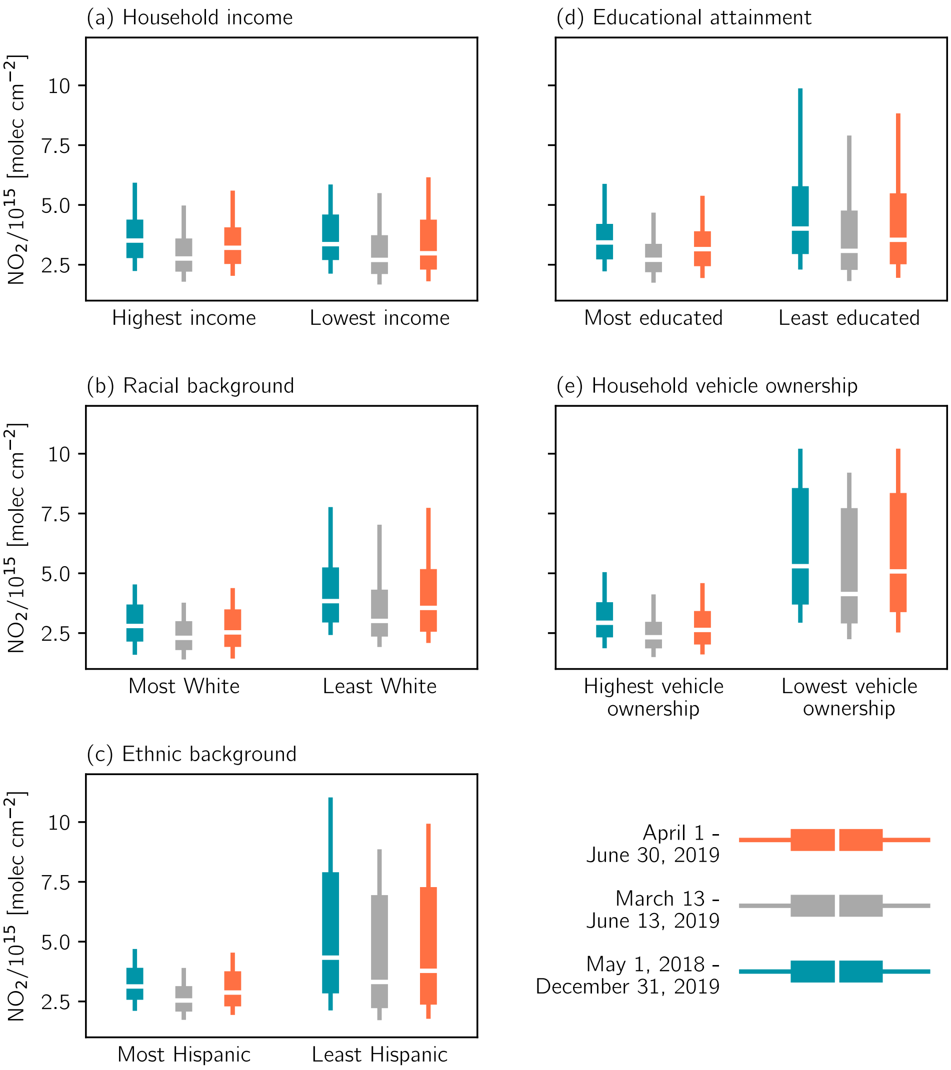

FIGURE 3. **Sensitivity of urban NO_2 disparities to the baseline period.** Extreme values of each demographic variable (using the first and tenth deciles) for three different baseline periods: 1 April - 30 June 2019, 13 March - 13 June 2019 (the period used in the main text), and 1 May 2018 - 31 December 2019 (the entire TROPOMI data record). Boxes extend to the lower and upper quartiles of the data, and the median value is indicated with the horizontal white lines. The lower and upper whiskers extend to the 10th and 90th percentiles, respectively.

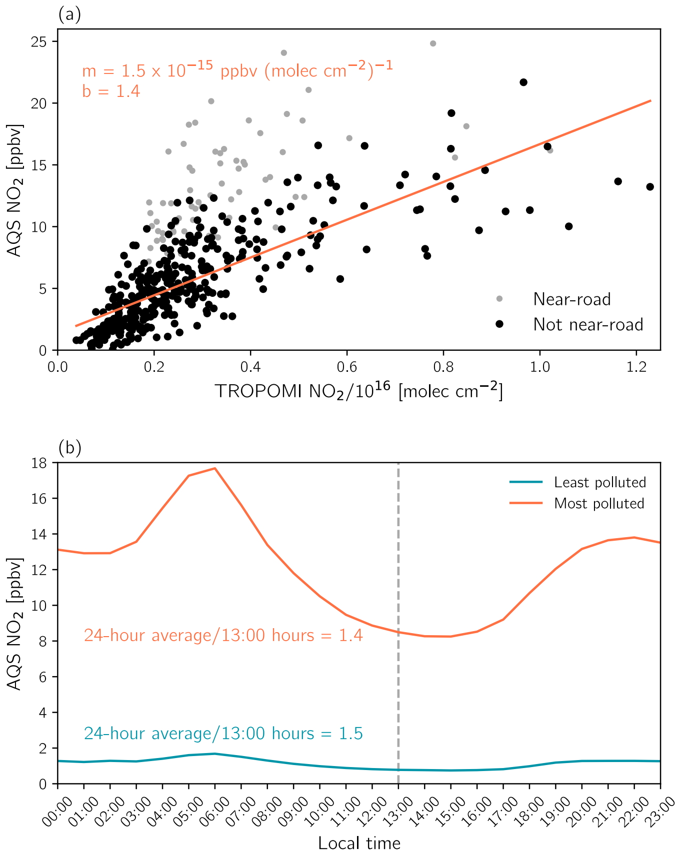

FIGURE 4. (a) Observed NO_2 from AQS monitors versus TROPOMI tropospheric NO_2 columns for the baseline period (13 March - 13 June 2019). TROPOMI data correspond to the nearest $0.01°$ latitude $\times$ $0.01°$ longitude grid cell to each AQS monitor. The orange line represents the linear regression fitted only through AQS data not flagged as "near-road" ($<$ 20 meters). The orange text gives the slope (m) and intercept (b) of this linear fit. (b) Observed diurnal cycles of NO_2 averaged over the most polluted (AQS monitors where the collocated TROPOMI grid cell $>$ 90th percentile) and least polluted sites (AQS monitors where the collocated TROPOMI grid cell $<$ 10th percentile) during the baseline period. Only sites that are not near-road are considered for these averages. The ratios of 24-hour average NO_2 to NO_2 at the approximate time of satellite overpass (dashed grey line; $\sim$ 13:00 hours local time) are indicated in the colored text.